Effect of transition metals and homogeneous hydrogen producers in the hydrothermal liquefaction of sewage sludge

Claudia Prestigiacomo [a,*], Joscha Zimmermann [b], Ursel Hornung [b], Klaus Raffelt [b], Nicolaus Dahmen [b], Onofrio Scialdone [a], Alessandro Galia [a]

[a] Dipartimento di Ingegneria, Sezione Chimica Ambientale Biomedica Idraulica e dei Materiali, Università degli Studi di Palermo, Viale delle Scienze, 90128 Palermo, Italy
[b] Institute of Catalysis Research and Technology (IKFT), Karlsruhe Institute of Technology, Eggenstein-Leopoldshafen 76344, Germany

ARTICLE INFO

Keywords:
Hydrothermal liquefaction
Biocrude
Metals
Hydrogen donor
Sewage sludge
Waste biomass

ABSTRACT

Hydrothermal liquefaction (HTL) of sewage sludge (SS) was performed in the presence of metallic Zn, Fe and Ni to investigate their effect on the performances of the process in terms of product yields and quality. Experiments were performed in subcritical water at 350 °C for 10 min using each metal individually and in the presence of homogenous hydrogen producers like formic acid (FA) and KOH. Interesting results were obtained with Zn that when used alone or in the presence of KOH, increased the cumulative biocrude (BC) yields and resulted in energy recoveries (ER) higher than 100% with respect to initial energy content of the biomass, thus indicating that HTL of SS is globally endothermic. Moreover, when Zn was used with FA it strongly enhanced gas yield leading to a significant hydrogen production that was determined to be generated mainly from SS or water. Ni chips were used in two consecutive HTL experiments with no decrease in BC yields and ER. Collected results suggest that metallic powders can be interesting catalyst to improve yield and quality of BC in particular when FA acid was used as hydrogen vector.

1. Introduction

Hydrothermal treatments are considered a promising route to convert carbonaceous matrices into value added materials [1–3]. Among these processes, hydrothermal liquefaction (HTL) was studied in the work herein. HTL consists of a thermochemical treatment of the carbonaceous matrix (bio-feedstock) in the presence of a proper solvent, usually water [3]. The process produces an oil phase, commonly defined as biocrude (BC), a gas phase, an aqueous phase, and a solid residue [3]. HTL is carried out at a temperature between 300 and 400 °C and pressure between 10 and 40 MPa [3–6]. Analyzing the recent literature on the field it is possible to observe that the operative conditions (reaction temperature and time) can be tuned depending on the treated bio-feedstock to maximize the yield of BC [3]. Microalgae are the most studied carbonaceous matrix [7], even if their utilization on the large scale is hindered by the high cost of production [8]. Moreover, virgin BC has a high S, N and O content that reduces its HHV and increases hydrophilicity, making the oil not compatible with fuel regulations. Heteroatoms must be removed by up-grading and the cost of the treatment would decrease if HTL could be performed limiting their presence in the BC. It was demonstrated that catalytic systems are needed to improve the BC quality, however it was not possible to find a catalytical active system with a long-term stability [9–11]. It seems also, that molecular hydrogen improves the BC quality [10,12]. In that framework, it was demonstrated that the utilization of a liquid hydrogen donor instead of molecular hydrogen is very promising because hydrogen is produced directly in the reaction medium minimizing gas-liquid mass transfer resistances [13]. Formic acid (FA), acetic acid, tetralin and ethanol were adopted in the literature as liquid hydrogen donors [10,14,15]. Some researchers found that KOH, if added to the HTL reactor could allow a faster depolymerization of biofeedstock. This effect was explained because KOH catalyze hydrogen production through homogeneous water gas shift reaction as reported by Sinag et al. [16], Kruse et al. [17] and Demirel et al. [18]. Waste carbonaceous matrices, such as sewage sludge (SS) seem to have a great potential, because they are namely costless matrices compared to the microalgae and HTL can be considered an interesting route to dispose them [15,19–22]. However, SS are characterized by high amount of non-biogenic fractions, such as salts,

* Corresponding author.
E-mail address: claudia.prestigiacomo01@unipa.it (C. Prestigiacomo).

Table 1
List of properties of SS provided from WWTP of Karlsruhe.

Proximate analysis (% *w*/w dry basis)	
Organic content (550 °C)	60 ± 3
Elemental analysis	
C	29.2 ± 0.2
H	4.8 ± 0.2
N	4.3 ± 0.2
S	1 ± 0.2
HHV (MJ/kg)[a]	13
Al	1.12 ± 0.4
Ca	3.66 ± 0.3
Fe	7.32 ± 1.1
K	< 0.9
Mg	0.38 ± 0.1
Na	< 0.46
P	3.59 ± 0.6
Ti	0.12
Zn	0.08
Si	3.39 ± 0.7

[a] Estimated using Dulong's formula as reported in the analytical methods section.

metals and plastics [23]. In particular SS contains a high amount of inorganics [22], such as Al, Ba, Ca, Cr, Cu, Fe, Ni, K, Mg, Mn, Na, P, S, Ti, Zn, Si which are distributed in the products at the end of the experiment. Metals are present in the aqueous stream at the entrance of the wastewater treatment plant and they are recovered with SS as waste to be disposed of. The presence of heavy metals represents a big challenge for the implementation of HTL on the industrial scale as they can affect product quality and/or the performances of the process. One of the hurdles of the transfer of the process from the lab to an industrial plant fed by SS is represented by the fact that the metals in the SS can be transferred to the BC affecting its placing on the market because some of them are toxic or they can poison the catalysts used in the hydrotreating processes of BC [24]. Some studies analyzed the distribution of metals in the phases produced by HTL of real SS and the main evidence was that the higher the reaction temperature, the higher is the fraction of metals entrapped in the produced BC [22,24–26]. However, metals can positively affect the process behavior acting as catalysts or heterogeneous additives [22]. Elemental Fe and Zn could react with sub/supercritical water and promote the production of molecular hydrogen inside the reactor [27–29].

Instead, Ni, Ti, Co, Mo, were extensively used to produce metal-based catalysts for HTL of biomass or upgrading of BC [29–32]. In this context, the nature of the carbonaceous matrix has been deeply investigated to comprehend how the elemental metals can affect the performances of the process in terms of product yields or quality. Among the several metals contained in residual biomass [10,24,25], Ni, Zn and Fe were selected as elemental model compounds. In this work a systematic investigation was conducted to study their effect individually and combine them with homogenous hydrogen producer as FA and KOH to evaluate for the first time their effect on the BC yield and quality.

2. Materials and methods

SS was provided by the wastewater treatment plant (WWTP) of Karlsruhe (Germany), with an initial moisture content of 75%*w*/w. In Table 1 the main properties of the SS used in this study are listed.

The raw SS was dried at 105 °C for 72 h, then milled with a pulverisette 14, Fritsch instrument to obtain particle dimensions between 0.1 and 0.2 mm. The ash content was determined by gravimetric analyses after calcination at 550 °C for 6 h and the organic content as the difference.

Potassium hydroxide (KOH, Analytical grade purity, Acros Organics) and formic acid (FA, 98–100% *w*/w Fluka) were used as homogeneous additives.

Metallic nickel (Ni, Alfa Aesar, 99.7%, metal basis, powder, 50 + 100 mesh, chips of metallic Ni, 1 mm width* 0.1–0.3 mm thickness), iron (Fe, Across Organics, 99%, metal basis, powder, 70 mesh) and zinc (Zn, Alfa Aesar, 99.9%, metal basis, powder, 100 mesh) were used to perform selected HTL experiments using deionized water as solvent. Acetone (≥ 97%, VWR) and cyclohexane (≥ 99.5% HiPerSolv CHROMANORM®) were used to recover the produced BC.

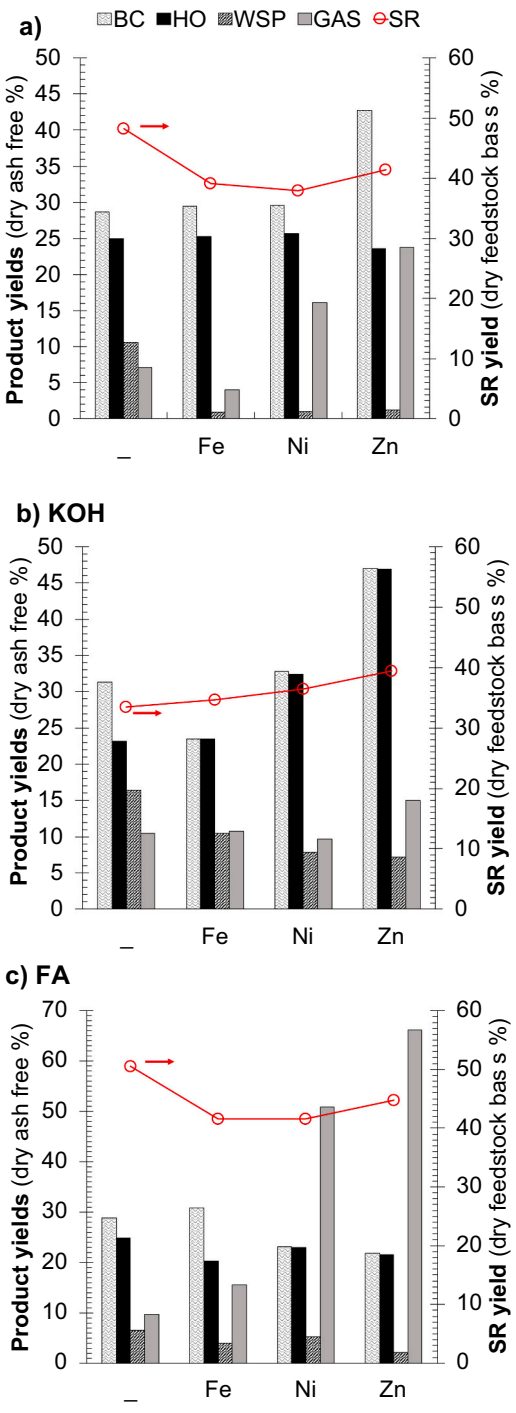

Fig. 1. Product yields obtained from HTL experiments conducted at 350 °C, 10 min in the presence of Fe, Ni and Zn metal powder; without homogeneous additives (a); with KOH (b); with FA (c).

2.1. Hydrothermal liquefaction

A home built AISI 316Ti autoclave batch reactor with an internal volume of 25 mL was used to perform HTL experiments at 350 °C and 10

Table 2
Gas phase composition obtained from HTL experiments conducted at 350 °C, 10 min in the presence of Fe, Ni and Zn metal powder; without homogeneous additives; with KOH; with FA.

Compound					KOH				FA			
	_	Fe	Ni	Zn	_	Fe	Ni	Zn	_	Fe	Ni	Zn
Ethylene	0.7	0.6	0.6	0.2	0.6	0.8	0.9	0.3	0.9	0.5	0.5	0.1
Ethane	0.4	0.3	0.4	0.2	0.3	0.3	0.5	0.2	0.3	0.1	0.1	0.1
Propylene	0.8	0.8	0.8	0.4	1.3	0.6	0.7	0.4	1.4	0.5	0.5	0.2
Propane	0.5	0.4	0.5	0.2	0.3	0.4	0.5	0.2	0.2	0.1	0.1	0.1
Methane	1.9	1.6	2.3	1.2	4.9	3.3	5.3	1.9	1.6	0.8	0.5	0.6
i-butane	0.2	0.1	0.2	0.1	0.3	0.1	0.2	0.1	0.1	0.0	0.0	0.0
n-butane	0.3	0.3	0.3	0.2	0.5	0.3	0.4	0.2	0.2	0.1	0.1	0.1
CO_2	94.0	94.6	94.0	46.2	91.2	93.9	91.1	44.7	80.0	62.7	73.5	44.5
H_2	ND	ND	ND	50.8	ND	ND	ND	51.7	9.3	31.0	15.5	54.0
CO	1.1	1.3	0.9	0.5	0.5	0.4	0.4	0.3	6.2	4.1	9.3	0.3

ND: not detected.

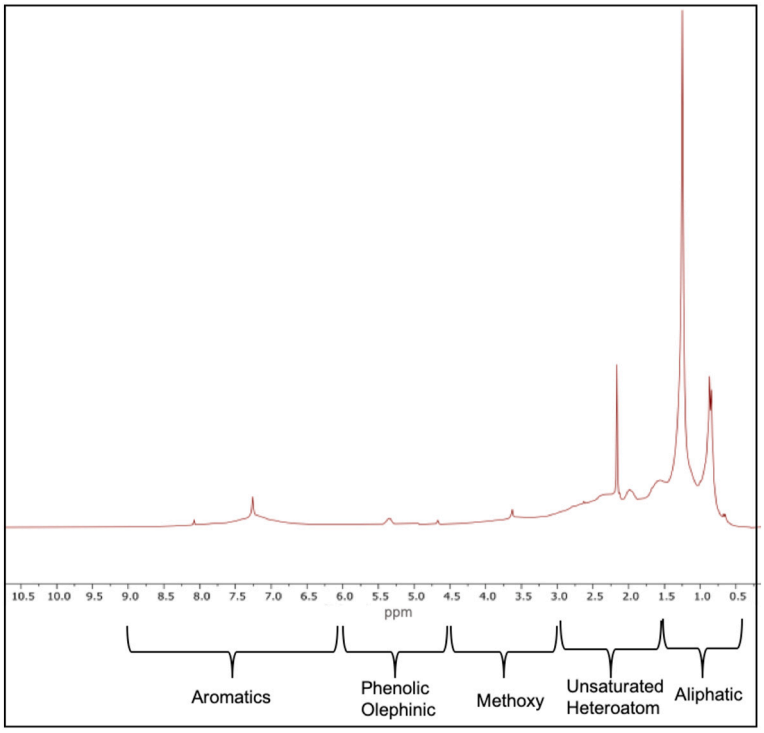

Fig. 2. Proton distribution obtained by ^{1}H NMR analysis of the HO from HTL of SS at 350 °C for 10 min, in the presence of Zn metal powder.

min as reaction temperature and time respectively. 10 g of an aqueous slurry at 10% *w*/w of dry SS were used as feedstock and each time Fe, Ni or Zn alone or in mixture with homogeneous FA and KOH were added to the slurry. The concentration of metals and homogeneous additives was 10% *w*/w related to the dry SS. With the loading of water adopted in this study at the reaction temperature of 350 °C about 62% of the reactor volume is filled with liquid water [19] and the pressure inside the reactor can be estimated as the vapor pressure of water that is close to 16.5 MPa [33]. In the presence of FA, the initial pH of the solution was around 2.2, this value became 13.3 with KOH. The reactor was purged with nitrogen (99.998% AirLiquide) to minimize its oxygen content before HTL leaving a residual pressure of 0.2 MPa. A fluidized sand bath was used to heat the reactor up to the reaction temperature. In this work, the heating profile inside the reactor was preliminary measured in a different but geometrically similar reactor equipped with a thermocouple and loaded with 10 g of pure water (i.e., the same amount of solvent used in HTL experiments). The average heating rate was 35 °C/min up to 300 °C and decreased to 3 °C/min up to 350 °C, so that the global heating time to reaction temperature is about 25 min. A holding time of 10 min was selected and considered to start when the set-up temperature was reached. At the end of each test the reactor was taken from the sand bath and put in cold water to cool down and stop the HTL reaction. Then the reactor was placed in a pre-evacuated chamber, it was opened, and the expansion of gases was induced. The gas phase quantification was made through the displacement of the water level due to accumulation of gases inside a graduated funnel connected to the pre-evacuated chamber. Gas phase composition was determined by GC-TCD/FID analyses of samples of 100 μL of gas phase.

2.2. *Product separation and analytical methods*

The procedures adopted for product separation were the same of those used in a previous investigation [10,19]. Briefly, after gas expansion the liquid products were collected in a centrifuge tube and 2 mL of cyclohexane were added to the tube to separate the BC from the aqueous phase. The reactor was washed with 10 mL of cyclohexane and the recovered liquid phase was poured into the centrifuge tube. The tube was centrifuged at 3220 rpm for 20 min. The supernatant liquid phase,

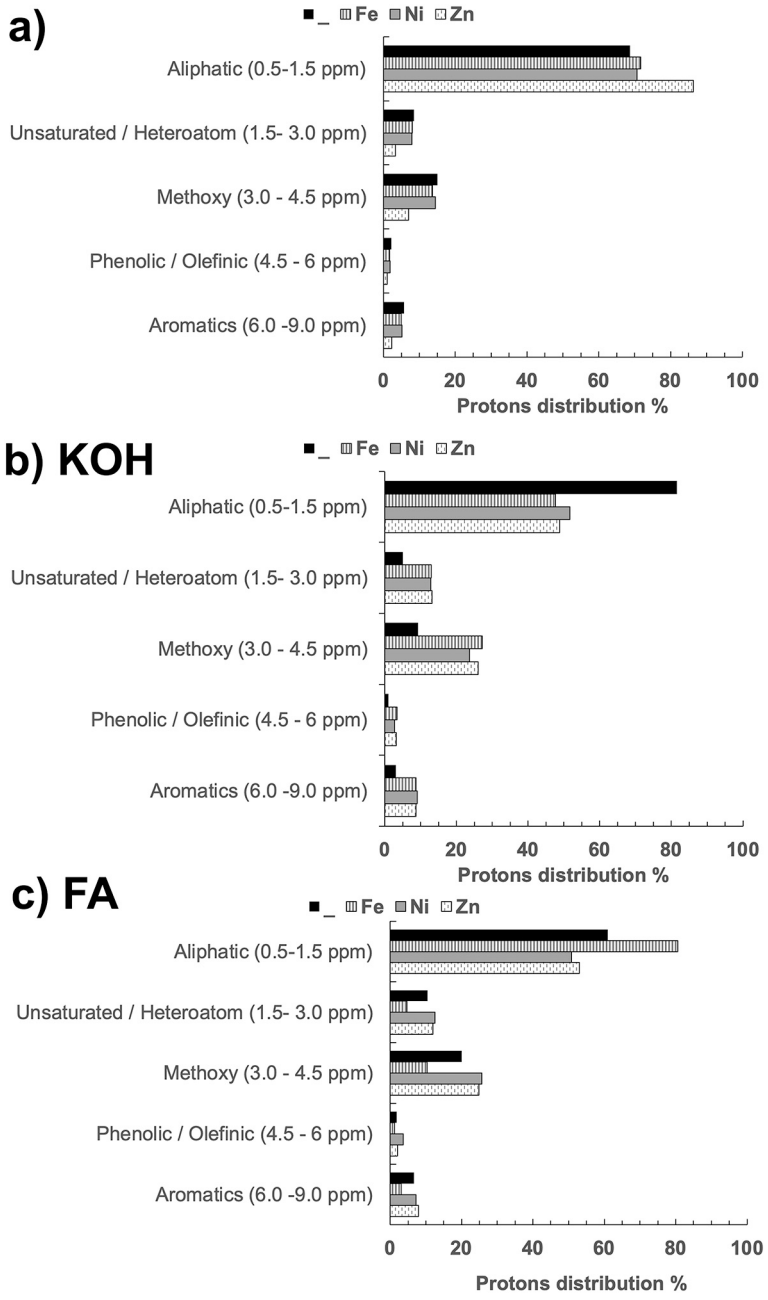

Fig. 3. ^{1}H NMR analyses of BC obtained from HTL experiments conducted at 350 °C, 10 min in the presence of Fe, Ni and Zn metal powder; without homogeneous additives; with KOH; with FA.

made of cyclohexane and solubilized BC was separated from the solids using a Pasteur pipette and stored in a round bottom flask. The aqueous phase was collected and stored in a glass vial and the water-soluble products (WSP) were estimated by gravimetric analyses. The reactor was washed several times with acetone to recover the residual BC and solid residue (SR). The suspended phase recovered with acetone was poured in the aforementioned round bottom flask and its content was filtered under vacuum using a Whatman nylon membrane with pore diameter of 0.45 μm. The SR was collected in the filter and dried for further gravimetric analyses. The filtrated liquid phase containing BC was subjected to a controlled evaporation process of the solvents as described by Prestigiacomo et al. [10,19], to collect a residual heavy oil phase (HO) from the round bottom flask, quantified by weighting, and a trapped liquid phase rich in re-condensed solvents. Gas chromatographic analyses of the trapped liquid phase were performed, and an additional hydrocarbon fraction (HC) was detected and quantified by calibration with standards. BC was considering as a summation of the quantified HO and HC mass.

2.3. Analytical methods

Initial moisture of SS and organic content of the dried organic matrix were determined by gravimetric analyses. Elemental analyses of the dry organic matrices were performed to determine carbon (C), hydrogen (H), nitrogen (N) and sulfur (S) content by Elementar vario MICRO cube. Oxygen content (% *w*/w) was determined by difference (Eq. (1)).

$$O \quad 100 \quad C \quad H \quad N \quad S \quad ash \tag{1}$$

where C, H, N, S are the % w/w detected by the elemental analyzer and ash is the average percentage of the calcinated samples (6 h at 550 °C).

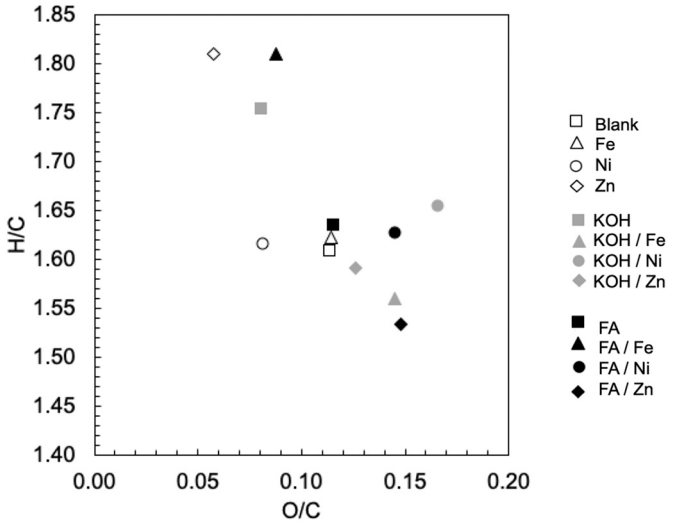

Fig. 4. Van Krevelen diagram of BC produced from HTL experiments conducted at 350 °C, 10 min in the presence of Fe, Ni and Zn metal powder; without homogeneous additives; with KOH; with FA.

All HTL experiments were repeated twice to determine the reproducibility and reported yields are mean values. The mean values of standard deviation (i.e., percentage value of the deviation of product yields) are reported as follows: 4.0% for BC, 3.9% for SR, 0.2% for WSP and 4.7% for gas. The yields of HO, HC, WSP and Gas ($Y_{product}$(%)) are calculated according to Eq. (2) in the dry ash free form (daf):

$$Y_{product}(\%w/w) \quad M_{p(daf)}/M_{b(daf)} \times 100 \tag{2}$$

where $M_{p(daf)}$is the dry ash free mass of each product and $M_{b(daf)}$ means the dry ash free mass of biofeedstock initially loaded into the reactor.

SR yield was calculated using dry SS basis, following the Eq. (3):

$$Y_{SR}(\%w/w) \quad M_{SR(dry)}/M_{b(dry\ SS)} \times 100 \tag{3}$$

where $M_{SR(dry)}$ is the dry mass of SR and $M_{b(dry\ SS)}$ means the dry mass of biofeedstock initially loaded in the reactor. $M_{SR(dry)}$ was estimated by subtracting the mass of loaded metallic powder from the total mass of collected residue.

When formic acid was loaded into the reactor the $M_{b(daf)}$ and $M_{b(dry\ SS)}$ included the mass of the acid since FA itself reacts in hydrothermal environment. The BC yield was determined as the summation of HO and HC yields.

In order to check BC quality in terms of H/C and O/C molar ratios, elemental analyses of BC samples were performed and HC identification in the liquid cold phase was achieved through gas chromatography analysis. The standard errors in the measurement of C, H, N and S % *w*/w were: 0.14%, 0.09%, 0.60% and 0.03% respectively. The high heating values (HHV) of BC were calculated by the expanded Dulong formula [34] in Eq. (4):

$$\text{HHV (MJ/kg)} \quad 0.338\text{C} + 1.44(\text{H–O}/8) + 0.094\text{S} \tag{4}$$

where C, H, O and S are the cumulative elemental % w/w determined in the HO through elemental analysis and in the HC fraction from its composition. The same calcination process used to determine the ash content in SS was performed on BC, SR and WSP. The calcination on the BC samples always found an ash percentage below detection limit (0.5% *w*/w). The liquid solutions recovered in the cold trap were analyzed using a Perkin Elmer Autosystem XL GC equipped with a capillary column ZB-FFAP (30 m * 0.25 mm * 0.25 mm) Phenomenex for C10-C18 hydrocarbon fractions, by an Agilent 7890B GC equipped with Stabilwax-DA 11023 column (30 m * 0.25 mm * 0.25 mm) for C4-C13 hydrocarbons. The oven programs used to conduct the analyses are:

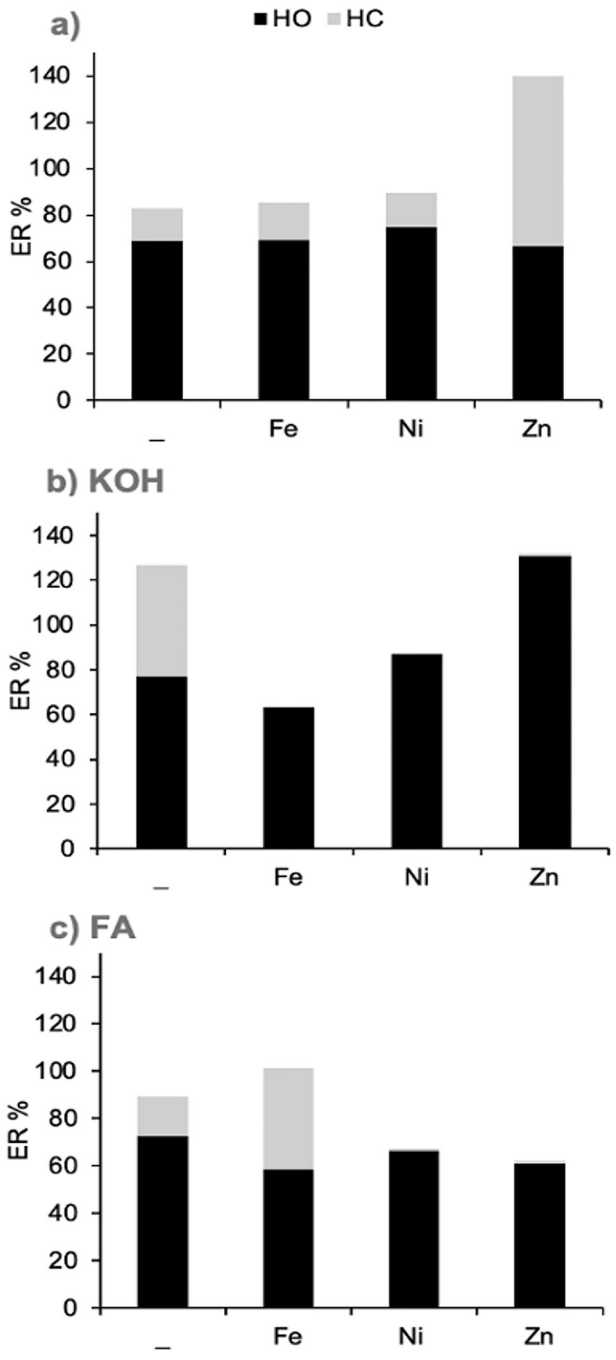

Fig. 5. ER % of the HO and of the HC. HTL experiments were conducted at 350 °C, 10 min in the presence of Fe, Ni and Zn metal powder; a) without homogeneous additives; b) with KOH; c) with FA.

- C10 C18 hydrocarbon fractions: 40 °C for 3 min, then 8 °C/min to 244 °C for 0 min maintaining 244 °C. 250 °C was the temperature at which the injector and the detector were set. The split ratio was 15:1, the He flow-rate in the column was 2.4 mL/min and 0.4 μL is the injection volume.
- C4 C13 hydrocarbon fraction: 40 °C for 10 min, then 8 °C/min to 250 °C for 10 min. 280 °C was the temperature of the detector. The split ratio was 10:1, He flow-rate in the column was 3 mL/min and 1 μL is the injection volume.

The identification and the calibration of the chromatograms were performed using GC analytical standards. The cumulative mass of HC

Table 3
Metal recovery MR (%) in the SR and in the AP produced from HTL experiments conducted at 350 °C, 10 min in the presence of Fe, Ni, Zn metal powder; without homogeneous additives; with KOH; with FA.

					KOH				FA			
	_	Fe	Ni	Zn	_	Fe	Ni	Zn	_	Fe	Ni	Zn
MR_{SR}	94.3	65.9	51.3	75.3	82.9	63.6	55.2	77.4	101.7	71.6	50.5	78.7
MR_{AP}	5.4	0.9	1.2	1.1	23.0	11.7	14.0	9.9	2.4	0.9	1.3	1.3
MR_{Total}	99.7	66.8	52.5	76.4	105.9	75.3	69.2	87.3	104.1	72.5	51.8	80.1

Table 4
Product yields obtained by HTL experiment conducted at 350 °C, 10 min, using chips or powder of Ni.

Homogeneous additive	Heterogeneous additive	Product yield (% *w*/w)				
		BC[a]	HC[a]	SR[b]	WSP[a]	GAS[a]
KOH	_	31	8	33	16	11
	Ni powder	32	<0.5	37	8	10
	Ni (Chips)	31	_	36	10	12
	Ni (R-Chips)[c]	34	_	31	9	12
FA	_	29	4	50	7	10
	Ni powder	23	<0.5	42	5	51
	Ni (Chips)	28	_	29	7	57
	Ni (R-Chips)[c]	30	_	28	2	58

[a] Dry ash free basis.
[b] Dry SS basis.
[c] Recycled chips.

detected in the liquid solution recovered in the cold trap was used to calculate the BC yield (as a sum of HO and HC mass to initial organic mass of SS loaded into the reactor).

Mol % of detected hydrocarbons was determined by the ratio between the mols of the identified hydrocarbon and the cumulative mols of all detected hydrocarbons per 100.

^{1}H NMR analyses of HO samples were performed to know the molar distribution of hydrogen atoms according to their nature and position in the molecules. The ^{1}H NMR analyses were recorded on a Bruker 250 MHz NMR spectrometer (Biospin 250). 0.1 g sample was dissolved in 0.7 ml of deuterated chloroform with tetramethyl silane as an internal standard. The solution was filtered through a 0.22 μm syringe filter (Spheros PFTE, LLG Labware), removing suspended particles. 1H spectra were acquired in 5 mm NMR tubes using a 90° pulse angle with a relaxation delay of 1 s, 126 accumulated scans and a spectral width of 3400 Hz. The resulting signals were processed and integrated with MestReNova 14.1.2. For the integration and functional group assignments, regions for the 1H spectra were given by Zimmermann et al. [35]. Signals from residual acetone and a trace of non-deuterated chloroform (δ 7.26 ppm) and their related areas were excluded by deconvolution. The HC composition in the liquid trapped phase was considered to estimate the molar distribution of methyl, methylene and olefinic hydrogen atoms in this fraction. The ^{1}HNMR and GC results were cumulated to obtain information representative of the BC product.

Inductively Coupled Plasma Mass Spectrometry (ICP-MS) analyses were performed with the native SS, the aqueous phase samples and the solid residues (SR) to detect the Al, Ba, B, Ca, Cu, Fe, K, Mg, Mn, Na, P, S, Si, Ti, Sr, F, Cl, Br, Zn and Ni contents. The metal recovery (MR) in the SR and aqueous phase (AP) was determined as follows:

$$MR_i(\%) \quad \left(\sum \omega_i M_p\right) \Big/ \left(\sum \omega_{i\,(SS)} M_{SS}\right) \times 100 \tag{5}$$

where i is the generic atom in SR or AP, $\sum\omega_i$ is the sum of the mass fraction of the metals in the product obtained by ICP analyses, M_p is the dry mass of recovered SR or AP, $\sum\omega_{i\,(SS)}$ is the sum of the mass fraction of the metals in the SS, M_{SS} is the dry mass of SS charged in the reactor. When metal powder was added to the reactor together with dry SS and water, $\sum\omega_i$ and $\sum\omega_{i\,(SS)}$ were calculated considering the mass of added powder. Chips of Ni were separated after SR recovery and for this reason their mass was not included in the MR calculation. MR calculations have a standard deviation of ±6.

The gas phase, taking samples of 100 μL, was analyzed by an Agilent 7890B Gas Chromatography equipped with a 2 m Molsieve 5 Å and 2 m Porapak Q column and through comparison with ethene, ethane, propylene, propane, methane, i-butane, n-butane, carbon dioxide, hydrogen and carbon monoxide standards and proper calibrations equations it was possible to obtain the volume percentage of each identified component in the analyzed sample. Ideal gas equation of state was then used to estimate the moles of produced gas phase. Triplicate injections were done to test the reproducibility of the results.

The energy recovery (ER) was used as a measure to evaluate the practical feasibility of the HTL of SS under the investigated operative conditions.

The ER of each collected product (ER_p) was estimated by the Eq. (6):

$$ER_p(\%) \quad \left[M^0_{tot} \times Y_p \times HHV_p \Big/ \left(m^0_{SS} HHV_{SS} + m^0_{FA} HHV_{FA}\right)\right] \times 100 \tag{6}$$

where M^0_{tot} is the total organic mass loaded in the reactor defined as sum of m^0_{SS} and m^0_{FA} that are respectively the initial organic mass of SS and of FA when used, Y_p is the product yield defined in Eq. (2), HHV_{SS} and HHV_{FA} are the high heating value of SS and FA respectively. HHV_{FA} was calculated with Eq. (4) knowing that the elemental composition of pure FA is 26.10% of C, 4.38% of H and 46.02% of O.

3. Results and discussions

3.1. Effect of transition metals and hydrogen producer additives

A reference experiment of HTL of SS was performed at 350 °C and 10 min, without addition of metals or homogeneous additives. A sample of BC produced by this experiment was analyzed through ICP analysis to search for the presence of metals finding 0.50%*w*/w of Fe, 0.18 of P %w/

Table 5
Metal recovery MR (%) in the SR and in the AP produced from HTL experiments conducted at 350 °C, 10 min in the presence of Ni metal powder, Chips of Ni, and reused chips (R-chips) of Ni; without homogeneous additives; with KOH; with FA.

	Blank[a]	KOH				FA			
		_	Ni powder	Ni chips	Ni R-chips[b]	_	Ni powder	Ni chips	Ni R-chips[b]
MR_{SR}	94.3	82.9	55.2	67.7	58.7	101.7	50.5	46.0	49.5
MR_{AP}	5.4	23.0	14.0	16.4	2.7	2.4	1.3	2.7	5.6
MR_{tot}	99.7	105.9	69.2	84.1	61.3	104.1	51.8	48.7	55.1

[a] Blank experiments without FA, KOH and metals.
[b] R-chips: reused chips.

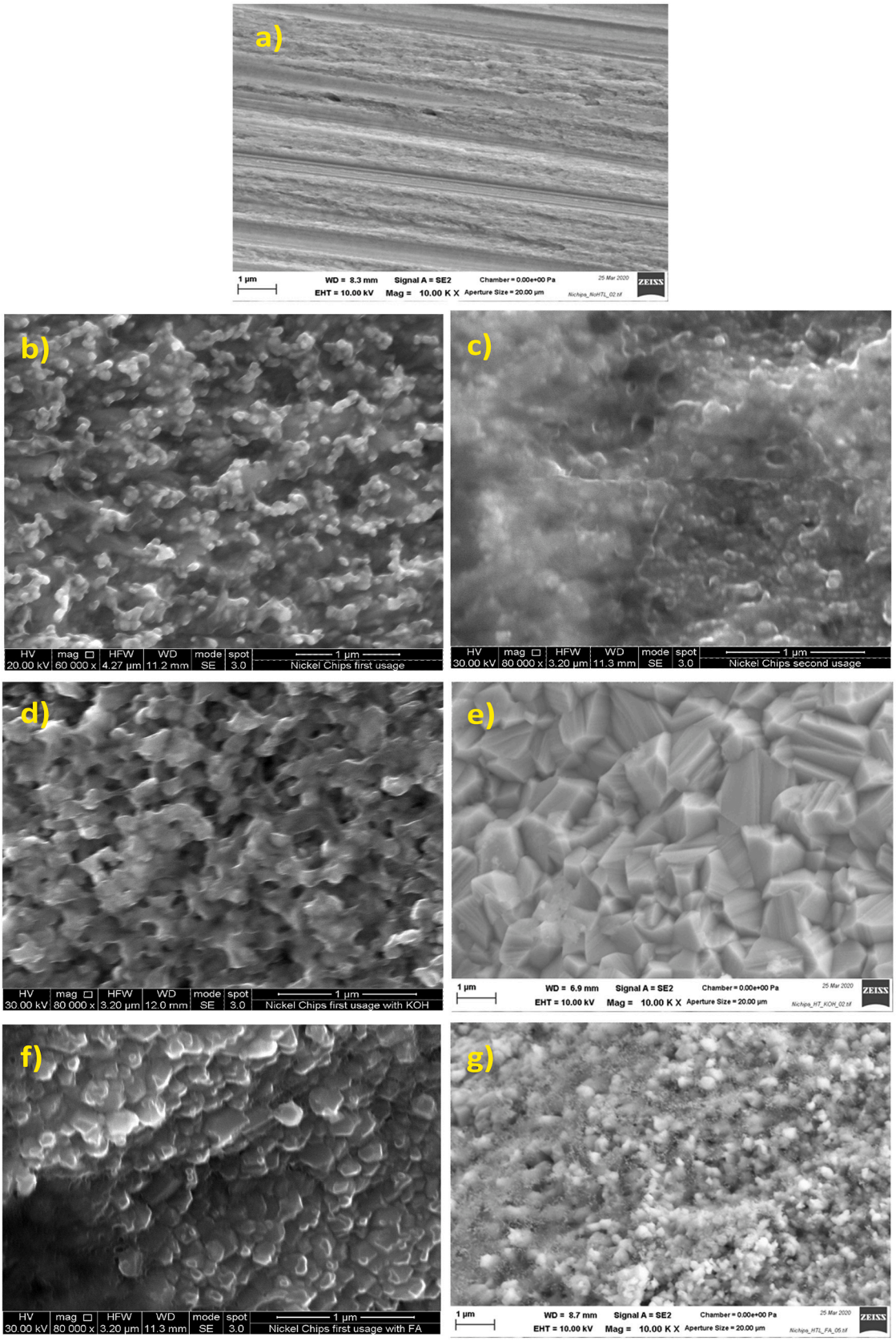

Fig. 6. SEM characterization of Ni surface. a) initial; b) after a first cycle of HTL without additives; c) after a second cycle of HTL without additives; d) after a first cycle of HTL in the presence of KOH; e) after a second cycle of HTL in the presence of KOH; f) after a first cycle of HTL in the presence of FA; g) after a second cycle of HTL in the presence of FA.

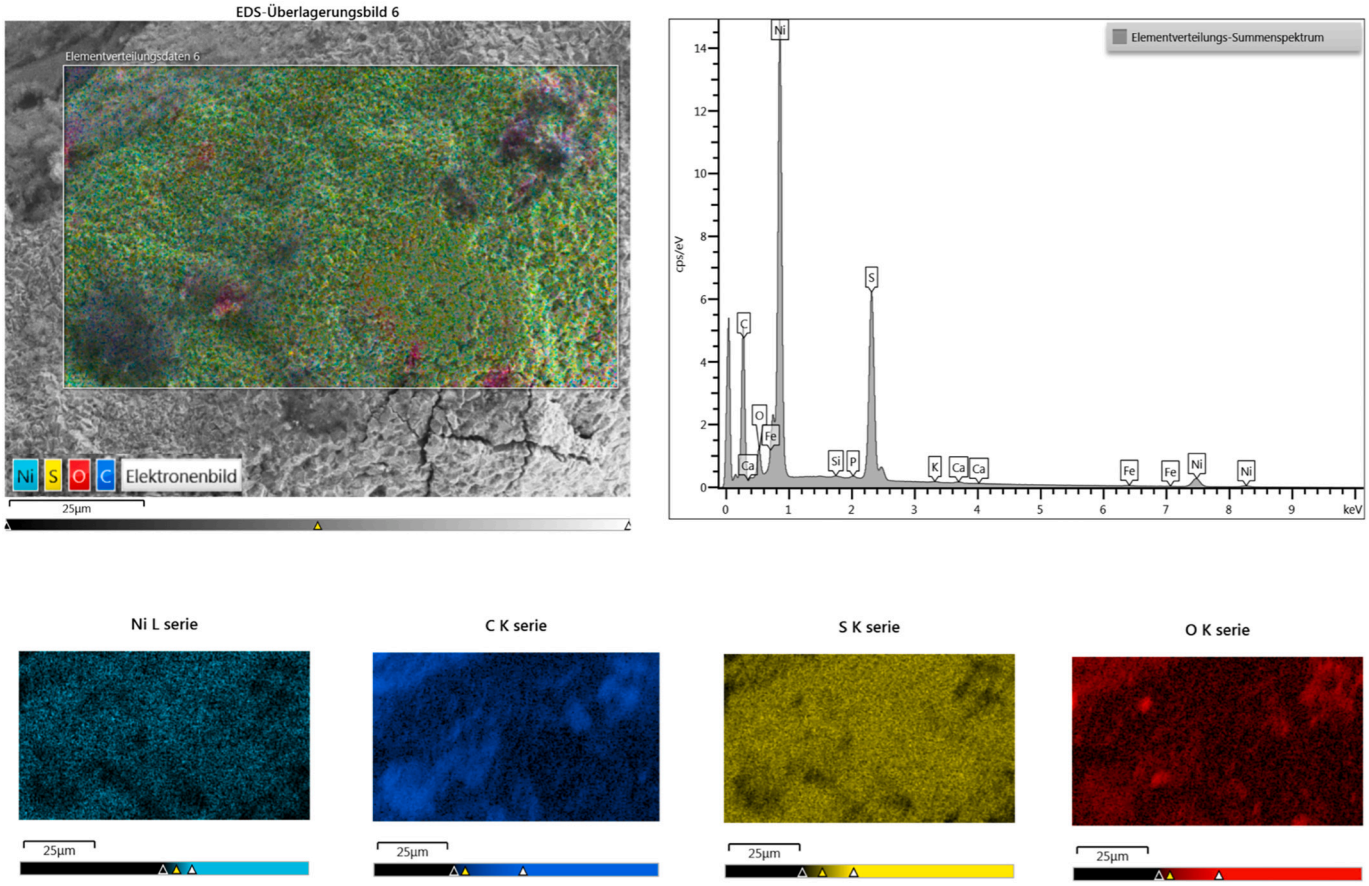

Fig. 7. SEM/ EDX analysis of reused Ni chips in the presence of KOH as additive.

w, 0.09%w/w of Al and Ca, 0.01%w/w of Zn. Then experiments in the presence of Fe, Ni and Zn metal powders (10%w/w related to dry SS) were performed and the main obtained results are reported in Fig. 1.

In the presence of added Fe and Ni, the BC and HC yields only marginally increased with respect to that measured with original SS. Differently, a strong increase of the cumulative yield of BC was observed when Zn powder was used (Fig. 1a), mainly due to a marked enhancement in HC production that reached a yield of 20%. In this fraction it was possible to detect the presence of C5, C6, C14, C16 alkanes which mol% were respectively 0.01, 0.13, 6.38 and 93.48.

The addition of transition metals decreased the yield in SR and WSP. Ni and Zn increased the yield in gas products that were constituted for more than 50% mol/mol by hydrogen when the less noble metal was used probably because of water reduction promoted by Zn oxidation according to reaction (7) [36]:

$$Zn + H_2O \leftrightarrows ZnO + H_2 \quad (7)$$

The enhancement in hydrogen production was not observed with iron because with this metal has been reported that the particle surface is soon covered by a passivating layer of hematite that prevents further reaction with water [28].

The same set of experiments was repeated adding KOH and FA as homogeneous additives. Also, in the presence of the alkaline compound the highest cumulative BC yields was obtained in the presence of Zn but, under these conditions, the HC fraction yield was below 0.5% and the higher oil production corresponded to generation of larger amount of HO fraction (Fig. 1b). Fe and Ni did not show evident beneficial effect on the cumulative BC yields. Again, in these sets of experiments added metals decreased the amount of WSP even if the effect was less marked than that observed in the additive-free experiments. The formation of HC compounds was not detected suggesting that KOH inhibits the hydrodeoxygenation effect of the metals.

When the transition metals were used with FA, cumulative BC yields were slightly improved only in the presence of Fe because of larger HC formation. When Ni and Zn metal powders were used cumulative BC yields were decreased to less than 20% and gasification prevailed (Fig. 1 c) as demonstrated by the gas yield that increased from 7-15% to 50–66%. In all experiments with Zn hydrogen was detected as the main component of the gas mixture and its concentration increased to 15% and 31% mol/mol also with Ni and Fe respectively when FA was added.

It is known that hydrogen can be produced above 320 °C by thermal decomposition of the formic acid, following the decarboxylation reaction pathway described elsewhere [37–39] and reported below:

$$HCOOH \rightarrow CO_2 + H_2 \quad (8)$$

To assess this hypothesis the stoichiometric amount of hydrogen from complete decomposition of FA was compared with that produced in the HTL experiment. When Zn was added to the reactor, only 14% of the produced hydrogen can be covered by the decomposition of FA, the residual moles coming from water or from organic molecules Table 2.

HO samples were analyzed by ^{1}H NMR and elemental analyzer to investigate the effect of metals and additives on the in-situ upgrading of the produced BC. Results of ^{1}H NMR spectra were analyzed dividing the proton signals according to their position in the molecules constituting the HO as follows:

- H $_{aromatic}$: hydrogen linked to aromatic ring incorporated in HO compounds (identified from 9 to 6.0 ppm);
- H $_{phenolic/olefinic}$: hydrogen in the hydroxyl group of phenols (represented at 5.4 ppm) together with hydrogen of unsaturated C═C bond represented by a triplet at 5.0–4.9 ppm (identified in the region from 6.0 to 4.5 ppm);

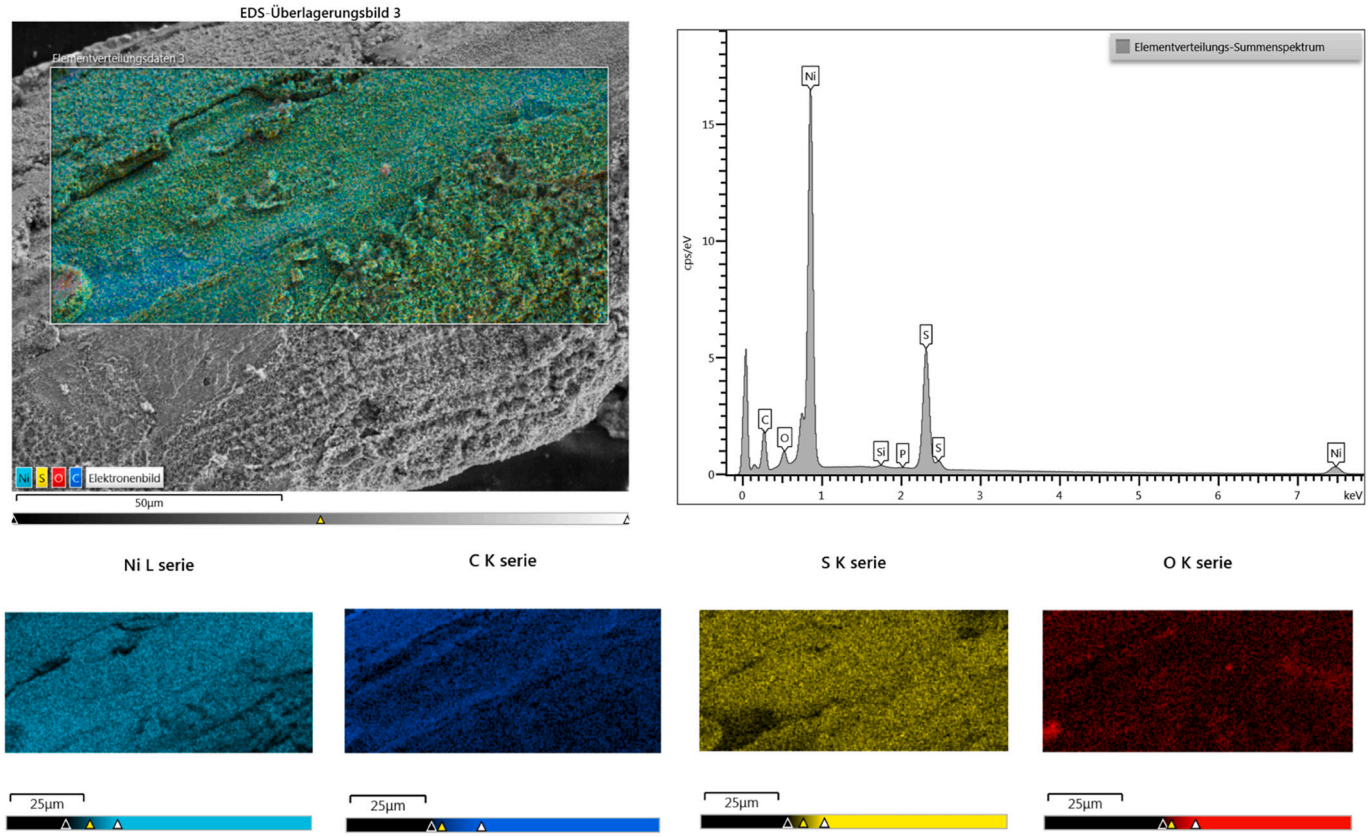

Fig. 8. SEM/ EDX analysis of reused Ni chips in the presence of FA as additive.

- H $_{methoxy}$: hydrogen in methoxy groups located at 3.6 ppm in the region 4.5–3.0 ppm [38];
- H $_{unsaturated/heteroatom}$: protons in α-position (1.5–1.8 ppm) and β-position (1.9–3.0 ppm) in N- and O-containing functional groups like linear or branched amides and non-aromatic heterocyclic compounds (identified from 3 to 1.5 ppm) [39];
- H $_{aliphatic}$: paraffinic methyl and methylene hydrogens (identified from 1.5 to 0.5 ppm);

In Fig. 2 the proton signal distribution is reported. In Fig. 3 the cumulative distribution of protons of BC are plotted determined combining the results of ^{1}H NMR and elemental analysis with the GC analysis of the HC fraction. From Fig. 3 we found that in BC obtained with Zn the fractions of hydrogen in α-position with respect to carbonyl and aromatic rings and that of aromatic protons were strongly depleted while the fraction of aliphatic hydrogen increased from 52 to 68%. These results clearly indicate that Zn promote hydrogenation and deoxygenation reactions and is confirmed by the elemental analysis reported in the Van Krevelen diagram (Fig. 4). The values of H/C and O/C of BC change from 1.61 to 1.81 and from 0.13 to 0.06 respectively when Zn was added to the reaction mixture. These improvement in the BC quality and yield led to a cumulative ER (as determined by Eq. (6)) significantly higher than 100% (Fig. 5), as already observed in our previous study that gave evidence of endothermic reactions involved in the HTL of SS [19] suggesting that beside the energy content of the biomass also the enthalpy used to drive the HTL can be stored in the BC. Also, when Zn was used with KOH and Fe together with FA, the ER were higher than 100% because of the high BC yield. In the latter case, this effect was accompanied by an increase of H/C and a reduction of O/C.

In general elemental composition data reported in the Van Krevelen diagram are in good agreement with ^{1}H NMR data thus supporting the validity of this approach to obtain a more resolved information on the quality of the BC. In fact, BC samples obtained with Zn and KOH alone and with Fe and FA in Fig. 3 are characterized by the highest fractions of aliphatic protons and lowest fractions of unsaturated/heteroatoms, methoxy, phenolic/olefinic and aromatic protons in agreement with their high H/C and low O/C.

SR and AP were characterized through ICP analyses (Tables S1 and S2). In Table 3 it is possible to observe the results in terms of metal recovery (MR %) in the products.

Most of the metals are recovered in the SR, however when initial metals were added, the cumulative percentage recovered in the SR and AP is strongly lower than 100%, indicating that metals can be present in the BC probably complexed by oxygenated and nitrogenated compounds.

3.2. *Ni reuse and characterization*

Among the tested metals, Ni was never detected in the aqueous phase and it is the metal with the highest standard reduction potential, that makes it more resistant to oxidation in water. For this reason in the work herein further experimentation conducted to study the stability of metals in two consecutive HTL experiments was performed with Ni. Since it was not possible to recover metal powders from the SR with adopted separation procedures, Ni metal powder was substituted by chips in this part of the study. The main obtained results are showed in Table 4.

When Ni powder was substituted with Ni chips BC yield was substantially unchanged in the presence of KOH and increased from 23 to 28% in the presence of FA. This effect on the yield can be due to the fact that chips of nickel were better distributed in the reaction medium owing to their filament like geometry and the active surface can be more available for the HTL reactions with respect to the nickel powder that is placed on the bottom of the static reactor mixed with solid components and then with a less accessible surface. Ni chips recovered and used for a second test gave BC yields of 34 instead of 31% with KOH and of 30

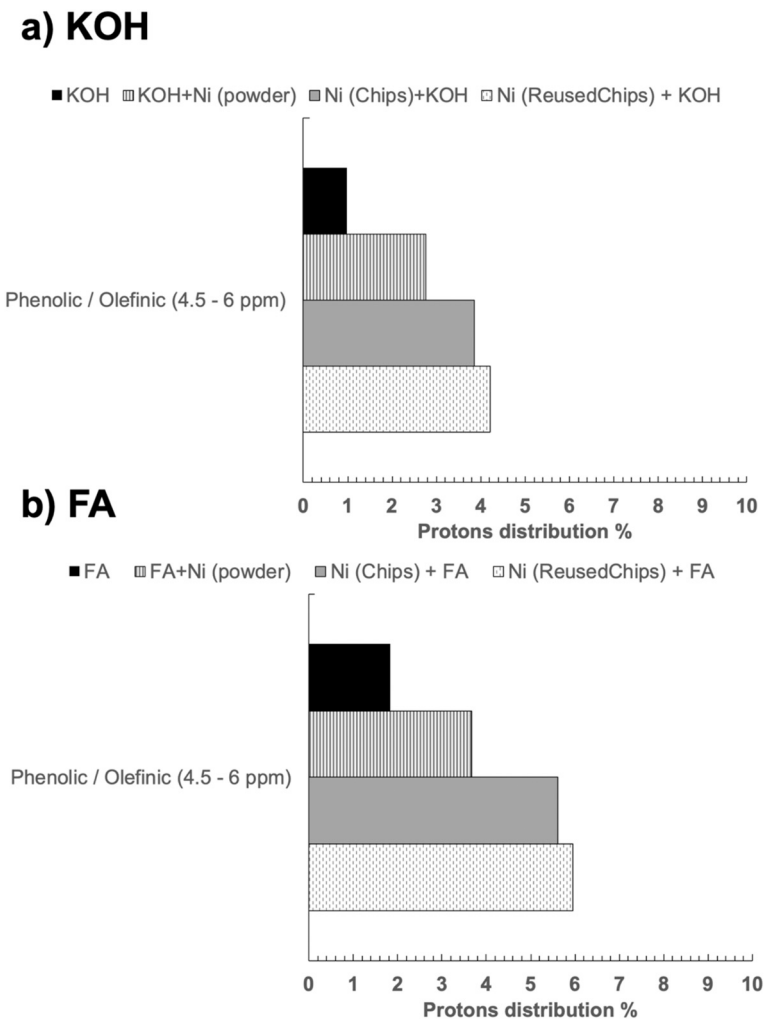

Fig. 9. ^{1}H NMR results of BC produced from HTL experiments conducted at 350 °C, 10 min in the presence of Ni metal powder, Chips of Ni, and reused chips of Ni; a) with KOH; b) with FA.

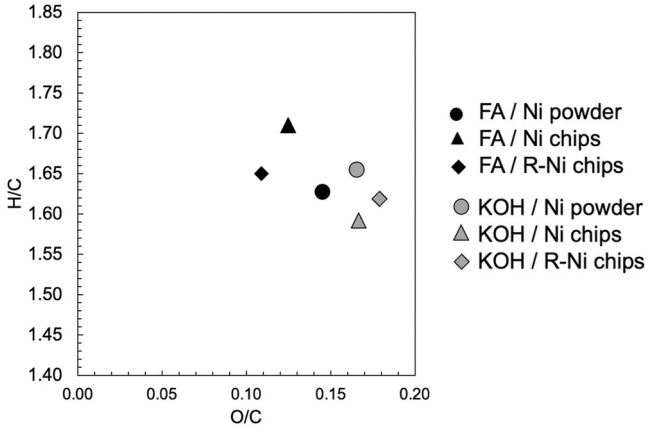

Fig. 10. Van Krevelen diagram reporting H/C and O/C molar ratio of BC produced from HTL experiments conducted at 350 °C, 10 min in the presence of Ni metal powder (Ni powder), chips of Ni (Ni chips) and reused chips of Ni (R-Ni chips); in the presence of KOH or FA.

instead of 28% with FA.

Looking at the BC quality we found that Ni chips gave H/C and O/C values reasonably similar to those obtained with powder. Another important figure of merits of the HTL process, the energy recovery ER, did not decrease when chips were reused that is another indication that Ni performances did not change after the 1st utilization. SR and WSP were analyzed by ICP (Tables S1 and S2) and Ni concentration in these fractions was below the detection threshold that indicates of the stability of this metal under hydrothermal condition (Table 5). Ni chips were characterized by SEM-EDX before and after their 1st utilization. Native chips had a layered compact surface. Used chips exhibited a modified surface morphology both in the absence and in the presence of KOH and FA (Fig. 6). Nickel chips tested alone and in the presence of formic acid revealed a hemispherical conical surface morphology. Moreover, in the presence of KOH surface structure with polygonal texture with well-defined facets was observed. Ni-S was reported to be active in the decarbonylation of carboxylic acids to olefins and in the hydro-deoxygenation of fatty acids to paraffins [40]. EDX analyses (Figs. 7 and 8 on the right side) showed the prevalence of the peak intensity of sulfur on the Ni surface recovered after the 1st HTL experiment and supports the findings of ^{1}H NMR results in Fig. 9 showing increasing abundance of olefinic protons. Higher fraction of olefinic hydrogen was observed with FA addition respect to KOH. Furthermore, Van Krevelen diagram in Fig. 10 showed as Ni chips with FA led to the production of a biocrude with relatively low O/C. This behavior was probably related to the role of FA as hydrogen vector in the reaction system. Furthermore, no negative effects were observed with Ni reutilization in the ER values of the biocrude (Fig. 11).

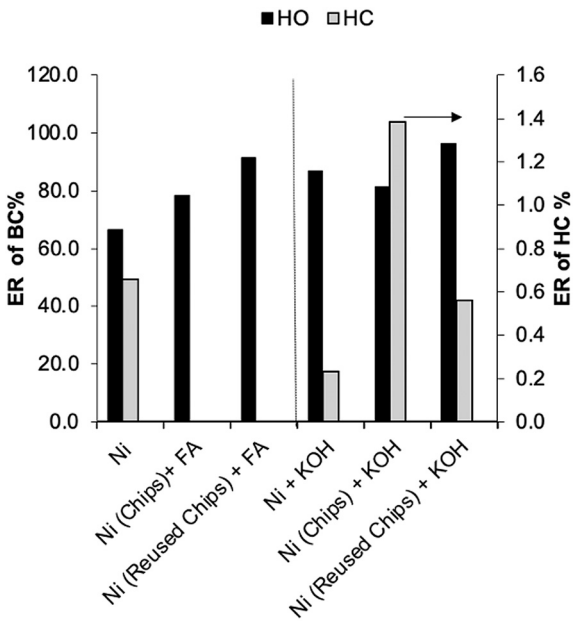

Fig. 11. ER % of HO and HC to study the effect of Ni chips. HTL experiments conducted at 350 °C, 10 min in the presence of Ni metal powder, Chips of Ni, and reused chips (R-chips) of Ni; without homogeneous additives; with KOH; with FA.

4. Conclusions

The effect of Fe, Ni and Zn alone and in the presence of FA and KOH as liquid hydrogen donors on the HTL of real SS was investigated. When Zn was used alone or in the presence of KOH increased the cumulative biocrude (BC) yields from 29 (blank experiment) to 43 and 48 respectively and resulted in energy recoveries (ER) higher than 100%, thus indicating that HTL of SS is globally endothermic. Moreover, when Zn was used with FA it strongly enhanced gas yield from 10 to 66% leading to a significant hydrogen production. Fe powders used in the presence of FA improved the quality and the energy recovery of BC. ICP analyses of the aqueous phase showed that Ni was not distributed in the aqueous phase, instead Zn complexes were found when FA or KOH were added to the HTL reactor. Ni chips were used in the place of powders in two consecutive HTL experiments with stable BC yields and ER. Collected results suggest that metallic powers can be interesting catalyst to improve yield and quality of BC in particular when FA acid was used as hydrogen vector.

CRediT authorship contribution statement

Claudia Prestigiacomo: Conceptualization, Investigation, Data curation, Writing – original draft. **Joscha Zimmermann:** Investigation. **Ursel Hornung:** Conceptualization, Writing – review & editing, Resources. **Klaus Raffelt:** Methodology, Validation. **Nicolaus Dahmen:** Writing – review & editing, Resources. **Onofrio Scialdone:** Writing – review & editing. **Alessandro Galia:** Visualization, Validation, Resources, Writing – review & editing.

Declaration of Competing Interest

The authors declare that they have no known competing financial interests or personal relationships that could have appeared to influence the work reported in this paper.

Acknowledgements

Italian Ministry of University, Italy, under project PON BIOFEEDSTOCK ARS01_00985 and Institute of Catalysis and Technology Research (IKFT), Karlsruhe Institute of Technology (KIT) are acknowledged for supporting and funding this work. We are grateful to Birgit Rolli, Sonja Habicht, Alexandra Bohm, Thomas Tietz and Dr. Michael Zimmermann from Institute of Catalysis and Technology Research (IKFT) for their skillful technical assistance.

Appendix A. Supplementary data

Supplementary data to this article can be found online at https://doi.org/10.1016/j.fuproc.2022.107452.

References

[1] S. Zinoviev, F. Müller-Langer, P. Das, N. Bertero, P. Fornasiero, M. Kaltschmitt, G. Centi, S. Miertus, Next-generation biofuels: survey of emerging technologies and sustainability issues, ChemSusChem. 3 (2010) 1106–1133, https://doi.org/10.1002/cssc.201000052.
[2] N. Kumar, A. Sonthalia, H.S. Pali, Sidharth, Next-Generation Biofuels—Opportunities and challenges, Green Energy and Technology, Springer Verlag (2020) 171–191, https://doi.org/10.1007/978-981-13-9012-8_8.
[3] A.A. Peterson, F. Vogel, R.P. Lachance, M. Froling, M.J. Antal, J.W. Tester, Thermochemical biofuel production in hydrothermal media: a review of sub- and supercritical water technologies, Energy Environ. Sci. 1 (2008) 32–65, https://doi.org/10.1039/b810100k.
[4] A. Dimitriadis, S. Bezergianni, Hydrothermal liquefaction of various biomass and waste feedstocks for biocrude production: a state of the art review, Renew. Sust. Energ. Rev. 68 (2017) 113–125, https://doi.org/10.1016/j.rser.2016.09.120.
[5] T.M. Yeh, J.G. Dickinson, A. Franck, S. Linic, L.T. Thompson, P.E. Savage, Hydrothermal catalytic production of fuels and chemicals from aquatic biomass, J. Chem. Technol. Biotechnol. 88 (2013) 13–24, https://doi.org/10.1002/jctb.3933.
[6] A. Demirbas, Biomass resource facilities and biomass conversion processing for fuels and chemicals, 2001, https://doi.org/10.1016/S0196-8904(00)00137-0.
[7] J. Yang, C. Hong, Y. Xing, Z. Zheng, Z. Li, X. Zhao, C. Qi, Research progress and hot spots of hydrothermal liquefaction for bio-oil production based on bibliometric analysis 28 (2021) 7621–7635, https://doi.org/10.1007/s11356-020-11942-2.
[8] A. Giaconia, G. Caputo, A. Ienna, D. Mazzei, B. Schiavo, O. Scialdone, A. Galia, Biorefinery process for hydrothermal liquefaction of microalgae powered by a concentrating solar plant: a conceptual study, Appl. Energy 208 (2017) 1139–1149, https://doi.org/10.1016/j.apenergy.2017.09.038.
[9] D. Castello, M.S. Haider, L.A. Rosendahl, Catalytic upgrading of hydrothermal liquefaction biocrudes: different challenges for different feedstocks, Renew. Energy 141 (2019) 420–430, https://doi.org/10.1016/j.renene.2019.04.003.
[10] C. Prestigiacomo, F. Proietto, V.A. Laudicina, A. Siragusa, O. Scialdone, A. Galia, Catalytic hydrothermal liquefaction of municipal sludge assisted by formic acid for the production of next-generation fuels, Energy 232 (2021), https://doi.org/10.1016/j.energy.2021.121086.
[11] L. Qian, S. Wang, P.E. Savage, Hydrothermal liquefaction of sewage sludge under isothermal and fast conditions, Bioresour. Technol. 232 (2017) 27–34, https://doi.org/10.1016/j.biortech.2017.02.017.
[12] K. Malins, V. Kampars, J. Brinks, I. Neibolte, R. Murnieks, R. Kampare, Biooil from thermo-chemical hydroliquefaction of wet sewage sludge, Bioresour. Technol. 187 (2015) 23–29, https://doi.org/10.1016/j.biortech.2015.03.093.
[13] A.F. Dalebrook, W. Gan, M. Grasemann, S. Moret, G. Laurenczy, Hydrogen storage: beyond conventional methods, Chem. Commun. 49 (2013) 8735–8751, https://doi.org/10.1039/c3cc43836h.
[14] A.B. Ross, P. Biller, M.L. Kubacki, H. Li, A. Lea-Langton, J.M. Jones, Hydrothermal processing of microalgae using alkali and organic acids, Fuel. 89 (2010) 2234–2243, https://doi.org/10.1016/j.fuel.2010.01.025.
[15] F. Lemoine, I. Maupin, L. Lemée, J.M. Lavoie, J.L. Lemberton, Y. Pouilloux, L. Pinard, Alternative fuel production by catalytic hydroliquefaction of solid municipal wastes, primary sludges and microalgae, Bioresour. Technol. 142 (2013) 1–8, https://doi.org/10.1016/j.biortech.2013.04.123.
[16] A. Sınag, S. Sınag, A. Kruse, J. Rathert, Influence of the Heating Rate and the Type of Catalyst on the Formation of Key Intermediates and on the Generation of Gases During Hydropyrolysis of Glucose in Supercritical Water in a Batch Reactor, 2004, https://doi.org/10.1021/ie030475.
[17] A. Kruse, D. Meier, P. Rimbrecht, M. Schacht, Gasification of pyrocatechol in supercritical water in the presence of potassium hydroxide, in: Industrial and Engineering Chemistry Research, ACS, 2000, pp. 4842–4848, https://doi.org/10.1021/ie0001570.
[18] E. Demirel, C. Erkey, N. Ayas, Supercritical water gasification of fruit pulp for hydrogen production: effect of reaction parameters, J. Supercrit. Fluids 177 (2021), https://doi.org/10.1016/j.supflu.2021.105329.
[19] C. Prestigiacomo, V.A. Laudicina, A. Siragusa, O. Scialdone, A. Galia, Hydrothermal liquefaction of waste biomass in stirred reactors: one step forward to the integral valorization of municipal sludge, Energy 201 (2020), https://doi.org/10.1016/j.energy.2020.117606.
[20] C. Prestigiacomo, P. Costa, F. Pinto, B. Schiavo, A. Siragusa, O. Scialdone, A. Galia, Sewage sludge as cheap alternative to microalgae as feedstock of catalytic

hydrothermal liquefaction processes, J. Supercrit. Fluids 143 (2019) 251–258, https://doi.org/10.1016/j.supflu.2018.08.019.
[21] A. Ali Shah, S. Sohail Toor, T. Hussain Seehar, K.K. Sadetmahaleh, T. Helmer Pedersen, A. Haaning Nielsen, L. Aistrup Rosendahl, Bio-crude production through co-hydrothermal processing of swine manure with sewage sludge to enhance pumpability, Fuel 288 (2021), https://doi.org/10.1016/j.fuel.2020.119407.
[22] Y. Zhai, H. Chen, B.B. Xu, B. Xiang, Z. Chen, C. Li, G. Zeng, Influence of sewage sludge-based activated carbon and temperature on the liquefaction of sewage sludge: Yield and composition of bio-oil, immobilization and risk assessment of heavy metals, Bioresour. Technol. 159 (2014) 72–79, https://doi.org/10.1016/j.biortech.2014.02.049.
[23] R. Chand, K. Kohansal, S. Toor, T.H. Pedersen, J. Vollertsen, Microplastics degradation through hydrothermal liquefaction of wastewater treatment sludge, J. Clean. Prod. 335 (2022), https://doi.org/10.1016/j.jclepro.2022.130383.
[24] H.J. Huang, X.Z. Yuan, The migration and transformation behaviors of heavy metals during the hydrothermal treatment of sewage sludge, Bioresour. Technol. 200 (2016) 991–998, https://doi.org/10.1016/j.biortech.2015.10.099.
[25] P. Manara, A. Zabaniotou, Towards sewage sludge based biofuels via thermochemical conversion - a review, Renew. Sust. Energ. Rev. 16 (2012) 2566–2582, https://doi.org/10.1016/j.rser.2012.01.074.
[26] L. Leng, X. Yuan, H. Huang, H. Jiang, X. Chen, G. Zeng, The migration and transformation behavior of heavy metals during the liquefaction process of sewage sludge, Bioresour. Technol. 167 (2014) 144–150, https://doi.org/10.1016/j.biortech.2014.05.119.
[27] B. de Caprariis, M. Scarsella, I. Bavasso, M.P. Bracciale, L. Tai, P. de Filippis, Effect of Ni, Zn and Fe on hydrothermal liquefaction of cellulose: Impact on bio-crude yield and composition, J. Anal. Appl. Pyrolysis 157 (2021), https://doi.org/10.1016/j.jaap.2021.105225.
[28] B. de Caprariis, I. Bavasso, M.P. Bracciale, M. Damizia, P. de Filippis, M. Scarsella, Enhanced bio-crude yield and quality by reductive hydrothermal liquefaction of oak wood biomass: effect of iron addition, J. Anal. Appl. Pyrolysis 139 (2019) 123–130, https://doi.org/10.1016/j.jaap.2019.01.017.
[29] B. de Caprariis, M.P. Bracciale, I. Bavasso, G. Chen, M. Damizia, V. Genova, F. Marra, L. Paglia, G. Pulci, M. Scarsella, L. Tai, P. de Filippis, Unsupported Ni metal catalyst in hydrothermal liquefaction of oak wood: effect of catalyst surface modification, Sci. Total Environ. 709 (2020), https://doi.org/10.1016/j.scitotenv.2019.136215.
[30] R. Bleta, B. Schiavo, N. Corsaro, P. Costa, A. Giaconia, L. Interrante, E. Monflier, G. Pipitone, A. Ponchel, S. Sau, O. Scialdone, S. Tilloy, A. Galia, Robust mesoporous CoMo/γ-Al2O3 catalysts from cyclodextrin-based supramolecular assemblies for hydrothermal processing of microalgae: effect of the preparation method, ACS Appl. Mater. Interfaces 10 (2018) 12562–12569, https://doi.org/10.1021/acsami.7b16185.
[31] R. Younas, S. Hao, L. Zhang, S. Zhang, Hydrothermal liquefaction of rice straw with NiO nanocatalyst for bio-oil production, Renew. Energy 113 (2017) 532–545, https://doi.org/10.1016/j.renene.2017.06.032.
[32] W. Tian, R. Liu, W. Wang, Z. Yin, X. Yi, Effect of operating conditions on hydrothermal liquefaction of Spirulina over Ni/TiO2 catalyst, Bioresour. Technol. 263 (2018) 569–575, https://doi.org/10.1016/j.biortech.2018.05.014.
[33] Joseph M. Smith, C. Hendrick, M.M. Abbott van Ness, Mark T. Swihart, Introduction to Chemical Engineering Thermodynamics, 2022.
[34] G. Marlair, C. Cwiklinski, A. Tewarson, An Analysis of Some Practical Methods for Estimating Heats of Combustion in Fire Safety Studies. https://hal-ineris.archives-ouvertes.fr/ineris-00972167, 2014.
[35] J. Zimmermann, K. Raffelt, N. Dahmen, Sequential hydrothermal processing of sewage sludge to produce low nitrogen biocrude, Processes 9 (2021), https://doi.org/10.3390/pr9030491.
[36] F.O. Ernst, A. Steinfeld, S.E. Pratsinis, Hydrolysis rate of submicron Zn particles for solar H2 synthesis, Int. J. Hydrog. Energy 34 (2009) 1166–1175, https://doi.org/10.1016/j.ijhydene.2008.11.098.
[37] T.M. McCollom, J.S. Seewald, Experimental constraints on the hydrothermal reactivity of organic acids and acid anions: I. Formic acid and formate, Geochim. Cosmochim. Acta 67 (2003) 3625–3644, https://doi.org/10.1016/S0016-7037(03)00136-4.
[38] Y. Yasaka, K. Yoshida, C. Wakai, N. Matubayasi, M. Nakahara, Kinetic and equilibrium study on formic acid decomposition in relation to the water-gas-shift reaction, J. Phys. Chem. A 110 (2006) 11082–11090, https://doi.org/10.1021/jp0626768.
[39] J. Yu, P.E. Savage, Decomposition of Formic Acid under Hydrothermal Conditions, Ind. Eng. Chem. Res. 37 (1998) 2–10, https://doi.org/10.1021/ie970182e.
[40] S. Brillouet, E. Baltag, S. Brunet, F. Richard, Deoxygenation of decanoic acid and its main intermediates over unpromoted and promoted sulfided catalysts, Appl. Catal. B Environ. 148–149 (2014) 201–211, https://doi.org/10.1016/j.apcatb.2013.10.059.